J|A|C|S
ARTICLES
Published on Web 06/18/2003

Enzyme Electrokinetics: Electrochemical Studies of the Anaerobic Interconversions between Active and Inactive States of *Allochromatium vinosum* [NiFe]-hydrogenase

Anne K. Jones,[†,§] Sophie E. Lamle,[†,§] Harsh R. Pershad,[†,§] Kylie A. Vincent,[†] Simon P. J. Albracht,[‡] and Fraser A. Armstrong*[,†]

Contribution from the Inorganic Chemistry Laboratory, Oxford University, South Parks Road, Oxford OX1 3QR, United Kingdom and Swammerdam Institute for Life Sciences, Biochemistry, University of Amsterdam, Plantage Muidergracht 12, NL-1018 TV Amsterdam, The Netherlands

Received March 24, 2003; E-mail: fraser.armstrong@chem.ox.ac.uk

Abstract: The cycling between active and inactive states of the catalytic center of [NiFe]-hydrogenase from *Allochromatium vinosum* has been investigated by dynamic electrochemical techniques. Adsorbed on a rotating disk pyrolytic graphite "edge" electrode, the enzyme is highly electroactive: this allows precise manipulations of the complex redox chemistry and facilitates quantitative measurements of the interconversions between active catalytic states and the inactive oxidized form Ni_r* (also called Ni−B or "ready") as functions of pH, H_2 partial pressure, temperature, and electrode potential. Cyclic voltammograms for catalytic H_2 oxidation (current is directly related to turnover rate) are highly asymmetric (except at pH > 8 and high temperature) due to inactivation being much slower than activation. Controlled potential-step experiments show that the rate of oxidative inactivation increases at high pH but is independent of potential, whereas the rate of reductive activation increases as the potential becomes more negative. Indeed, at 45 °C, activation takes just a few seconds at −288 mV. The cyclic asymmetry arises because interconversion is a two-stage reaction, as expected if the reduced inactive Ni_r−S state is an intermediate. The rate of inactivation depends on a chemical process (rearrangement and uptake of a ligand) that is independent of potential, but sensitive to pH, while activation is driven by an electron-transfer process, Ni(III) to Ni(II), that responds directly to the driving force. The potentials at which fast activation occurs under different conditions have been analyzed to yield the potential−pH dependence and the corresponding entropies and enthalpies. The reduced (active) enzyme shows a p*K* of 7.6; thus, when a one-electron process is assumed, reductive activation at pH < 7 involves a net uptake of one proton (or release of one hydroxide), whereas, at pH > 8, there is no net exchange of protons with solvent. Activation is favored by a large positive entropy, consistent with the release of a ligand and/or relaxation of the structure around the active site.

Introduction

The hydrogen cycle, in which H_2 is exploited as an initial electron donor while H^+ serves as a terminal electron acceptor, is a crucial feature of the metabolism of many prokaryotic and eukaryotic species.[1−3] Hydrogenases, the enzymes that catalyze the interconversions between H_2 and H^+, are classified into three groups: that is, [NiFe], [Fe], and those that do not contain a metal at the active site. These enzymes are targets for intense research activity, partly because of their technological potential as catalysts for the production of H_2 or its oxidation in fuel cells.[1] The [NiFe] enzymes function more effectively in the direction of H_2 oxidation. They contain, in addition to the buried Ni−Fe center, one or more Fe−S clusters that mediate long-range electron transfer. As a rule, the [NiFe]-hydrogenases are reversibly inactivated upon exposure to O_2 or other oxidants, with reactivation requiring reduction, typically by H_2.[4−14] X-ray diffraction studies in combination with infrared spectroscopy have revealed the structures of the Ni−Fe active site of closely related enzymes from different organisms and in different

[†] Oxford University.
[‡] University of Amsterdam.
[§] These authors contributed equally to this work.

(1) Cammack, R., Frey, M., Robson, R., Eds. *Hydrogen as a Fuel: Learning from Nature*; Taylor and Francis: London and New York, 2001.
(2) Vignais, P. M.; Billoud, B.; Meyer, J. *FEMS Microbiol. Rev.* **2001**, *25*, 455−501.
(3) Adams, M. W. W.; Mortenson, L. E.; Chen, J.-S. *Biochim. Biophys. Acta* **1981**, *594*, 105−176.
(4) Cammack, R.; Fernandez, V. M.; Hatchikian, E. C. *Methods Enzymol.* **1994**, *243*, 43−68.
(5) Albracht, S. P. J.; Kalkman, M. L.; Slater, E. C. *Biochim. Biophys. Acta* **1983**, *724*, 309−316.
(6) Fernandez, V. M.; Hatchikian, E. C.; Cammack, R. *Biochim. Biophys. Acta* **1985**, *832*, 69−79.
(7) Fernandez, V. M.; Hatchikian, E. C.; Patil, D. S.; Cammack, R. *Biochim. Biophys. Acta* **1986**, *883*, 145−154.
(8) Coremans, J. M. C. C.; van der Zwaan, J. W.; Albracht, S. P. J. *Biochim. Biophys. Acta* **1992**, *1119*, 157−168.
(9) Albracht, S. P. J. *Biochim. Biophys. Acta* **1994**, *1188*, 167−204.
(10) Mege, R.-M.; Bourdillon, C. *J. Biol. Chem.* **1985**, *260*, 14701−14706.
(11) Barondeau, D. P.; Roberts, L. M.; Lindahl, P. A. *J. Am. Chem. Soc.* **1994**, *116*, 3442−3448.
(12) Roberts, L. M.; Lindahl, P. A. *J. Am. Chem. Soc.* **1995**, *117*, 2565−2572.
(13) Carepo, M.; Tierney, D. L.; Brondino, C. D.; Yang, T. C.; Pamplona, A.; Telser, J.; Moura, I.; Moura, J. J. G.; Hoffman, B. M. *J. Am. Chem. Soc.* **2002**, *124*, 281−286.
(14) van der Zwaan, J. W.; Coremans, J. M. C. C.; Bouwens, E. C. M.; Albracht, S. P. J. *Biochim. Biophys. Acta* **1990**, *1041*, 101−110.

Scheme 1. Simplified Overview of the Spectroscopically Characterized States of the Ni−Fe Active Site of [NiFe]-hydrogenases[a]

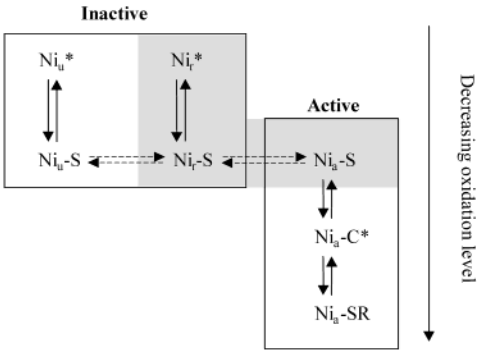

[a] Notation is as follows: "r" = "ready", "u" = "unready", and "a" = "active". EPR-silent states are designated "S", while EPR-detectable states are marked with *. Vertical transitions correspond to one-electron redox reactions when measured in the presence of redox-mediating dyes. In the absence of mediators, H_2 is in equilibrium only with the Ni_a-C^* and Ni_a-SR states. Alternative terminology has been used by different authors; the states may be translated as follows: $Ni_u^* = Ni-A$; $Ni_u-S = Ni-SI_u = Ni-SU$; $Ni_r^* = Ni-B$; $Ni_r-S = Ni-SI_r = Ni-SI$; $Ni_a-S = Ni-SI_a$; $Ni_a-C^* = Ni-C^*$; $Ni_a-SR = Ni-R$.

states.[15−22] However, the nature and mechanisms of these interconversions are not fully understood.

Scheme 1 summarizes the relationships between spectroscopically characterized states of the Ni−Fe active site.[23] There exist two, most oxidized, inactive, EPR-detectable states which are referred to as Ni_u^* and Ni_r^* (see Scheme 1 for alternative terminology): these both contain Ni(III) and Fe(II) but differ in that whereas Ni_u^* reacts with H_2 only after hours of incubation at ambient temperature (hence "u" for unready), Ni_r^* reacts within minutes (hence "r" for ready).[6] The states Ni_u^* and Ni_r^* can be converted in one-electron reactions to their respective reduced forms Ni_u-S and Ni_r-S, both of which are EPR-silent and catalytically inactive. At ambient temperatures or below, the Ni_u^*/Ni_u-S conversion is reversible, but the Ni_r^*/Ni_r-S conversion is not.[8] Above 30 °C, the Ni_u-S state converts to the Ni_r-S state (although this is slow). Under reducing conditions and again above 30 °C, Ni_r-S converts to the EPR-silent, active state Ni_a-S, which can then be reduced to the EPR-detectable Ni_a-C^* state.[25] When produced by incubating with H_2 in the absence of mediating redox dyes, the EPR signal

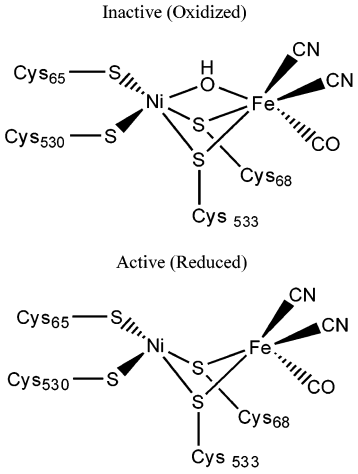

Figure 1. Structures of the catalytic center of [NiFe]-hydrogenases. The structure is based on the results of X-ray studies (ref 16) and FTIR spectroscopy (refs 17, 18, 33). The Ni−Fe site is attached to the protein through thiols from four Cys residues in the large subunit (residue numbers according to the *D. gigas* enzyme). The Fe ion coordinates the CN^- and CO ligands. In the *D.* gigas enzyme, the nonprotein bridging ligand is presumably a hydroxyl group. In the inactive state, the Fe ion is six-coordinate, while the Ni ion is five-coordinate. During the conversion between inactive oxidized and active reduced states, the Fe remains low-spin Fe(II), while the Ni changes between Ni(III) and Ni(II). In the active species (Ni_a-C^*) that is believed to be a catalytic intermediate, a bridging hydride ligand may be coordinated between the Ni and Fe atoms (Foerster, S.; Stein, M.; Brecht, M.; Ogata, H.; Higuchi, H.; Lubitz, W. *J. Am. Chem. Soc.* **2003**, *125*, 83−93).

of Ni_a-C^* is stable for hours after removal of H_2.[11,26,27] With excess H_2, it converts to the EPR-silent state Ni_a-SR. Each of the active states, Ni_a-S, Ni_a-C^*, and Ni_a-SR have been proposed to be involved in the catalytic cycle.[1,12,28−31]

The earlier-mentioned infrared and crystallographic studies provide important clues as to how these states differ in structure.[15−22] As shown in Figure 1, the Ni and Fe atoms in the active site are coordinated to the protein via four cysteinyl sulfurs: two are terminal ligands to the Ni atom, while the other two form a bridge between the Ni and Fe atoms. In addition, the Fe atom is coordinated by two CN^- ligands and a CO, which were identified by FTIR spectroscopy.[17,18,32,33] In aerobically prepared crystals, the Ni(III) and Fe(II) atoms are connected by an additional bridging ligand that is absent in structures of the reduced active protein and is thought to be an oxo or hydroxo species.[15,16,18,20,34] This suggests a structural reason for the oxidative inactivation, specifically, that the additional ligand produces a coordination which is unfavorable for the binding and activation of H_2. This is supported by spectroscopic (^{17}O EPR and ENDOR) studies.[13,14] Oxidation by $^{17}O_2$ of the H_2-reduced *Allochromatium vinosum* enzyme in H_2O or oxidation by $^{16}O_2$ of a sample of the enzyme from *Desulfovibrio gigas* in

(15) Volbeda, A.; Charon, M.-H.; Piras, C.; Hatchikian, E. C.; Frey, M.; Fontecilla-Camps, J. C. *Nature* **1995**, *373*, 580−587.
(16) Volbeda, A.; Garcin, E.; Piras, C.; De Lacey, A. L.; Fernandez, V. M.; Hatchikian, E. C.; Frey, M.; Fontecilla-Camps, J. C. *J. Am. Chem. Soc.* **1996**, *118*, 12989−12996.
(17) Happe, R.; Roseboom, W.; Pierik, A. J.; Albracht, S. P. J.; Bagley, K. A. *Nature* **1997**, *385*, 126.
(18) De Lacey, A. L.; Hatchikian, E. C.; Volbeda, A.; Frey, M.; Fontecilla-Camps, J. C.; Fernandez, V. M. *J. Am. Chem. Soc.* **1997**, *119*, 7181−7189.
(19) Higuchi, Y.; Ogata, H.; Miki, K.; Yasuoka, N.; Yagi, T. *Structure* **1999**, *7*, 549−556.
(20) Garcin, E.; Vernede, X.; Hatchikian, E. C.; Volbeda, A.; Frey, M.; Fontecilla-Camps, J. C. *Structure* **1999**, *7*, 557−566.
(21) Volbeda, A.; Montet, Y.; Vernède, X.; Hatchikian, E. C.; Fontecilla-Camps, J. C. *Int. J. Hydrogen Energy* **2002,** 27, 1449−1461.
(22) Ogata, H.; Mizoguchi, Y.; Mizuno, N.; Miki, K.; Adachi, S.; Yasuoka, N.; Yagi, T.; Yamauchi, O.; Hirota, S.; Higuchi, Y. *J. Am. Chem. Soc.* **2002**, *124*, 11628−11635.
(23) Happe, R. R.; Roseboom, W.; Albracht, S. P. J. *Eur. J. Biochem.* **1999**, *259*, 602−608. Albracht, S. P. J. In *Hydrogen as a Fuel: Learning from Nature*; Cammack, R., Frey, M., Robson, R., Eds.; Taylor and Francis: London and New York, 2001.
(24) Bleijlevens, B.; Faber, B. W.; Albracht, S. P. J. *J. Biol. Inorg. Chem.* **2001**, *6*, 763−769.
(25) Bleijlevens, B. PhD Thesis, University of Amsterdam, 2002.
(26) van der Zwaan, J. W.; Albracht, S. P. J.; Fontijn, R. D.; Slater, E. C. *FEBS Lett.* **1985**, *179*, 271−277.
(27) Coremans, J. M. C. C.; van Garderen, C. J.; Albracht, S. P. J. *Biochim. Biophys. Acta* **1992**, *1119*, 148−156.
(28) Maroney, M. J.; Bryngelson, P. A. *J. Biol. Inorg. Chem.* **2001**, *6*, 453−459.
(29) Siegbahn, P. E. M.; Blomberg, M. R. A.; Wirstam, M.; Crabtree, R. H. *J. Biol. Inorg. Chem.* **2001**, *6*, 460−466.
(30) Fan, H.-J.; Hall, M. B. *J. Biol. Inorg. Chem.* **2001**, *6*, 467−473.
(31) De Lacey, A. L.; Fernandez, V. M.; Rousset, M.; Cavazza, C.; Hatchikian, E. C. *J. Inorg. Biol. Chem.* **2003**, *8*, 129−134.
(32) Bagley, K. A.; van Garderen, C. J.; Chen, M.; Duin, E. C.; Albracht, S. P. J.; Woodruff, W. H. *Biochemistry* **1994**, *33*, 9229−9236.
(33) Bagley, K. A.; Duin, E. C.; Roseboom, W.; Albracht, S. P. J.; Woodruff, W. H. *Biochemistry* **1995**, *34*, 5527−5535.

the Ni_a-C^* state in $H_2{}^{17}O$ resulted in Ni_r^* and Ni_u^* states in which the unpaired spin of the Ni(III) ions showed hyperfine coupling to ^{17}O. This coupling was lost upon reductive activation. Structural differences between the active sites in the Ni_u^* and Ni_r^* states remain unclear, although it has been shown by EPR that the O-ligand is coordinated in a different manner in either state.[24]

Several methods are commonly used to measure hydrogenase activity.[1,4] These are as follows: (i) H_2 consumption or evolution is monitored manometrically in the presence of oxidized or reduced redox partners (e.g., cytochrome c_3 or viologens); (ii) electron consumption/production is monitored spectroscopically by following the state of redox indicators (e.g., methylene blue, benzyl viologen, or dichloro-indophenol (DCIP) for H_2 oxidation; reduced methyl viologen for H_2 production); (iii) electron consumption/production is measured amperometrically (the current is proportional to turnover rate) using a natural or artificial mediator such as cytochrome c_3 or viologens;[10,35,36] (iv) H/D exchange (H_2/D_2O or D_2/H_2O) is measured by mass spectrometry (in the absence of electron donors or acceptors) or, alternatively, tritium is used and the radioactivity is monitored; (v) conversion of *para* to *ortho* hydrogen is monitored by measuring thermal conductivity.

Protein film voltammetry (PFV), dynamic electrochemistry of protein molecules confined to an electrode surface, provides the means to study catalytic electron transfer (ET) activity of enzymes and makes possible the resolution of kinetics and underlying thermodynamics that may otherwise be highly convoluted.[37,38] There is direct exchange of electrons with the electrode surface; in other words, no mediators such as methyl viologen are used, so that the experiment can address the entire sample on a time scale that is effectively instantaneous. Provided supply of substrate to the electrode is not a limiting factor, and interfacial ET is sufficiently fast, the catalytic current is a direct measure of the enzyme's inherent activity.[39,40] The redox states of different centers and, correspondingly, the activities that may depend critically on these redox states are easily controlled and varied *directly* by applying the electrode potential over a continuous range. Consequently, it is possible to navigate among the different states of a complex system such as depicted in Scheme 1 and to determine, simultaneously, the thermodynamics and kinetics of the interconversions.

In an earlier study of *A. vinosum* (formerly known as *Chromatium vinosum*) [NiFe]-hydrogenase, we reported[41] that catalytic oxidation of H_2 under a partial pressure of 0.1 bar H_2 at 30 °C was extremely fast and efficient ($>1500\ s^{-1}$). More recently, we have shown how the activity of the Ni−Fe center compares favorably with that of a Pt catalyst[42] and determined some important yet subtle features of the mechanisms of proton reduction, H_2 oxidation, and interfacial electron transfer.[43,44] We have now exploited our ability to manipulate and control the enzyme's redox chemistry at an electrode in order to study the interconversions between active and inactive states of the Ni−Fe active site that occur under anaerobic conditions. The experiments provide insight and a quantitative framework to complement the information obtained from structural and spectroscopic methods.

Materials and Methods

The [NiFe]-hydrogenase from *A. vinosum* (*Av*H_2ase) was prepared as described previously.[8] Experiments were carried out in a glovebox (Vacuum Atmospheres or M. Braun) under an anaerobic N_2 atmosphere ($O_2 < 5$ ppm). The pyrolytic graphite edge (PGE) rotating disk electrode (area 3 mm^2) was constructed as described previously[45] and used in conjunction with an EG&G M636 electrode rotator. The all-glass electrochemical cell incorporated a three-electrode configuration and was equipped with an "o"-ring gasket that fitted snugly around the electrode rotator to seal the internal atmosphere from that of the glovebox. This allowed fast and precise variations in H_2 partial pressure, simply by exchanging the gas above the solution (Air Products, 100% H_2 or 1% H_2 in N_2) via inlet and outlet sidearms, and allowing 10 min for equilibration, during which time the electrode was rotated. A platinum wire was used as the counter electrode, and a saturated calomel electrode (SCE) in a Luggin sidearm containing 0.1 M NaCl was used as the reference. The reference potential was corrected with respect to the standard hydrogen electrode (SHE) by using $E_{SHE} = E_{SCE} + 242$ mV at 25 °C,[46] and all values given are with respect to SHE. (In this paper, we will frequently abbreviate potential as "*E*" and current as "i".) The main compartment was jacketed and thermostated at the desired experimental temperature, while the reference electrode sidearm was well separated and maintained at 25 °C. The configuration was thus nonisothermal, allowing equilibria at all temperatures to be referenced against a common standard, and no further corrections were made when calculating entropies and enthalpies.

Voltammetry and chronoamperometry were performed with an Autolab PGSTAT10 or PGSTAT20 electrochemical analyzer (Eco Chemie, Utrecht, The Netherlands) controlled by GPES software (Eco Chemie) and equipped with a digital (staircase) scan generator and an electrochemical detection (ECD) module for increased sensitivity. Cyclic voltammograms were recorded in the digital mode, with fractional sampling duration (α) = 0.5. In chronoamperometry experiments, the current was sampled every second following the potential step. Tests carried out without enzyme present showed that the initial decay in charging current following a potential step persisted for at least 10 s before dropping to a level where it could be ignored. This "slow charging effect" has been reported before for electrochemistry at PGE electrodes,[47] and although its amplitude was small (typically less than 1 μA for a step of 600 mV), the data collected for the first 10 s after the step were expected to be influenced. This period was therefore treated as a nominal "deadtime" and not given significance.

Experiments were performed using a mixed buffer system consisting of sodium acetate, MES (2-[*N*′-morpholino]ethane-sulfonic acid), HEPES (*N*′-[2-hydroxyethyl]piperazine-*N*′-[2-ethane-sulfonic acid]), TAPS (*N*′-tris[hydroxymethyl]methyl-3-amino-propane-sulfonic acid), and CHES (2-[*N*′-cyclohexylamino]ethane-sulfonic acid); all were purchased from Sigma, with final concentrations of 15 mM in each

(34) Stadler, C.; de Lacey, A. L.; Montet, Y.; Volbeda, A.; Fontecilla-Camps, J. C.; Conesa, J. C.; Fernandez, V. M. *Inorg. Chem.* **2002**, *41*, 4424−4434.
(35) Karyakin, A. A.; Varfolomeev, S. D. *Russ. Chem. Rev.* **1986**, 1524−1549.
(36) Moreno, C.; Franco, R.; Moura, I.; LeGall, J.; Moura, J. J. G. *Eur. J. Biochem.* **1993**, *217*, 981−989.
(37) Armstrong, F. A.; Heering, H. A.; Hirst, J. *Chem. Soc. Rev.* **1997**, *26*, 169−179.
(38) Armstrong, F. A. *J. Chem. Soc., Dalton Trans.* **2002**, 661−671.
(39) Heering, H. A.; Hirst, J.; Armstrong, F. A. *J. Phys. Chem. B* **1998**, *102*, 6889−6902.
(40) Léger, C.; Heffron, K.; Pershad, H. R.; Maklashina, E.; Luna-Chavez, C.; Cecchini, G.; Ackrell, B. A. C.; Armstrong, F. A. *Biochemistry* **2001**, *40*, 11234−11245.
(41) Pershad, H, R.; Duff, J. L. C.; Heering, H. A.; Duin, E. C.; Albracht, S. P. J.; Armstrong, F. A. *Biochemistry* **1999**, *38*, 8992−8999.
(42) Jones, A. K.; Sillery, E.; Albracht, S. P. J.; Armstrong, F. A. *J. Chem. Soc., Chem. Commun.* **2002**, 866−867.
(43) Léger, C.; Jones, A. K.; Albracht, S. P. J.; Armstrong, F. A. *J. Phys. Chem. B* **2002**, *106*, 13058−13063.
(44) Léger, C.; Jones, A. K.; Roseboom, W.; Albracht, S. P. J.; Armstrong, F. A. *Biochemistry* **2002**, *41*, 15736−15746.
(45) Sucheta, A.; Cammack, R.; Weiner, J. H.; Armstrong, F. A. *Biochemistry* **1993**, *32*, 5455−5465.
(46) Bard, A. J.; Faulkner, L. R. *Electrochemical Methods. Fundamentals and Applications*, 2nd edition; Wiley: New York, 2001.
(47) Hirst, J.; Armstrong F. A. *Anal. Chem.* **1998**, *70*, 5062−5071.

component and containing 0.1 M NaCl as an additional supporting electrolyte. All solutions were prepared with purified water (Millipore: 18 MΩ cm) and titrated with NaOH or HCl to the desired pH at the experimental temperature. To stabilize protein films, a coadsorbate, polymyxin B sulfate (Sigma) was added from a stock solution (10−20 mg ml^{-1}) to give a final concentration of 200 μg ml^{-1}. The pH values of final solutions were always checked after the experiment at the temperature used for measurements.

Prior to each experiment, the PGE electrode was polished with an aqueous alumina slurry (Buehler, 1 μm) and sonicated thoroughly. To prepare a protein film, the electrode was placed into a dilute enzyme solution (pH 7; 45 °C; 0.1−1.0 μM hydrogenase, containing polymyxin B sulfate) and kept stationary under N_2, while cycling the electrode potential between −558 mV and +242 mV versus SHE at 10 mV s^{-1} until a stable catalytic response was obtained, as described previously.[41] This typically requires 20 min, following which the electrode exhibits diffusion-controlled H_2 oxidation when H_2 is introduced to the cell. Such high activity presents a problem for studies designed to measure small changes in enzyme activity (diffusion control masks details of the catalytic properties of the enzyme). Therefore, after forming the film, the electrode was repolished with a damp cotton bud to lower the enzyme coverage, so that the catalytic current obtained in the presence of H_2 became independent of electrode rotation rate above 1500 rpm (see below). The cell solution was then replaced with an enzyme-free solution (ca. 5 mL); this avoids the problem of enzyme molecules on the electrode surface exchanging with enzyme molecules in solution, thereby corrupting the results. To ensure that any unready enzyme (Ni_u*) is activated,[9] the electrode with the enzyme film was then incubated for a further period of 1 h under 1 bar H_2 at 45 °C, with the electrode poised at −558 mV. Experiments were then commenced.

Comments on the Effect of Coverage of Hydrogenase on the Electrode. A film of *Av*H_2ase on a PGE electrode, prepared by adsorbing the enzyme to maximum electroactive coverage, displays an H_2-oxidation current that, at 45 °C, is sensitive to the electrode rotation rate even at high frequency under 1 bar hydrogen.[42] In other words, the oxidation rate is so fast that it is determined by H_2 mass transport to the electrode. The electroactive coverage (Γ) of the enzyme can, in principle, be determined from the area under nonturnover peaks that are attributed to the reversible redox transitions of the Fe−S clusters.[38−41] These nonturnover signals are faint for *Av*H_2ase and only observable in a limited number of experiments, suggesting an upper limit for Γ of 3 pmol cm^{-2}. Even so, such an "optimal" film can present a problem for studying the (in)activation of *Av*H_2ase because, even as most enzyme molecules become inactivated, the high overall activity of the film means that catalytic activity may still be controlled by H_2 transport to the electrode. This raises the likelihood that a partially active film of enzyme molecules will behave little differently to a film in which all enzyme molecules are active; that is, the current is not a linear function of the number of active sites. Consequently, after forming a film, the electrode was lightly polished to remove enzyme molecules and ensure a sufficiently low coverage that the current due to catalytic H_2 oxidation becomes rotation-rate *independent*, at least above a practical rotation rate such as 1500 rpm. The effect of enzyme coverage on the electrode rotation-rate dependence is predicted by the microscopic model.[48] At low coverage, the enzyme molecules lie at the loci of radial diffusion fields akin to a microelectrode array, and rotation-rate independent voltammetry is obtained. By contrast, with higher coverage films, the diffusion layers of the enzyme molecules overlap so that linear diffusion of substrate dominates, and the supply of substrate to each enzyme molecule is thereby less efficient leading to rotation-rate-dependent voltammetry.

Results

General Observations. Figure 2A and B shows cyclic voltammograms obtained at two different scan rates for a low

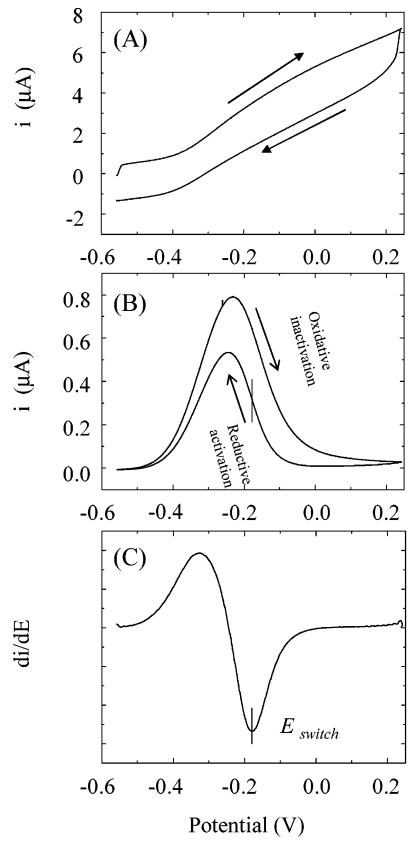

Figure 2. Cyclic voltammogram of a depleted film of *Av*H_2ase on a PGE electrode recorded at scan rates of (A) 200 mV s^{-1} and (B) 0.3 mV s^{-1} (arrows indicate the direction of potential cycling). The vertical bar on the curve (B) indicates the position of E_{switch}. Other conditions were temperature 48 °C, 1 bar H_2, pH 8.8, and electrode rotation rate 2500 rpm. (C) Derivative of the current/potential profile obtained during the reductive sweep of voltammogram B, showing the origin of E_{switch} as the local minimum in the high-potential region of the scan.

coverage film of *Av*H_2ase on a PGE electrode, catalyzing oxidation of H_2 (1 bar) at pH 8.8. The cycles have been initiated from a potential of −558 mV, and the electrode is rotating at 2500 rpm. At 48 °C, the response at a scan rate of 200 mV s^{-1} is sigmoidal-like, with the current due to H_2 oxidation increasing and beginning to level off as the potential becomes more positive. That the current does not level off completely is attributable to enzyme molecules that are not so well ET-coupled with the electrode and only contribute at higher driving force.[43] On the return sweep, as the potential is subsequently lowered, the catalytic H_2 oxidation current returns to a negligible level. Apart from changes in the background charging, the overall shape and current of the voltammogram are not significantly altered over scan rates ranging from 200 mV s^{-1} to greater than 10 V s^{-1}, showing that a steady state is achieved throughout these time domains. There is no rotation-rate dependence above 1500 rpm, as the coverage of enzyme has been lowered, and the results are reproducible provided the enzyme film has been "preactivated" under H_2 at 45 °C to activate Ni_u* (see Materials and Methods). Experiments performed under the same conditions with a bare PGE electrode (no enzyme film) show no H_2 oxidation current, thus confirming that catalysis is due entirely

(48) Armstrong, F. A.; Bond, A. M.; Büchi, F. N.; Hamnett, A.; Hill, H. A. O.; Lannon, A. M.; Lettington, O. C.; Zoski, C. G. *The Analyst* **1993**, *118*, 973−978.

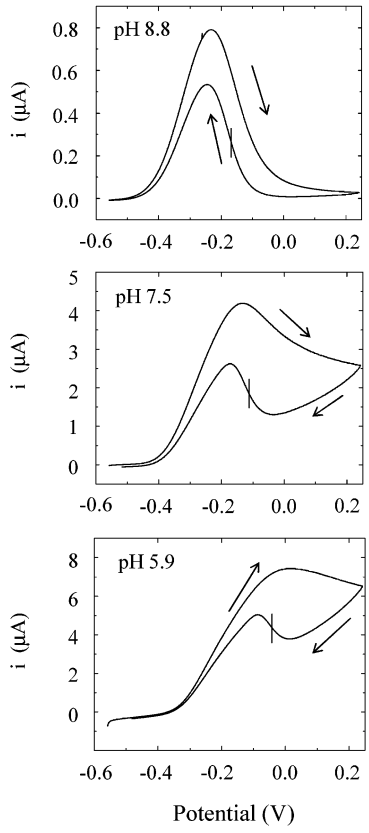

Figure 3. Cyclic voltammograms for a film of *Av*H_2ase measured at pH values as indicated. Arrows indicate the direction of the potential cycle. The vertical bar on the curves indicates the position of E_{switch}. Temperature 48 °C, 1 bar H_2, scan rate 0.3 mV s^{-1}, electrode rotation rate 2500 rpm.

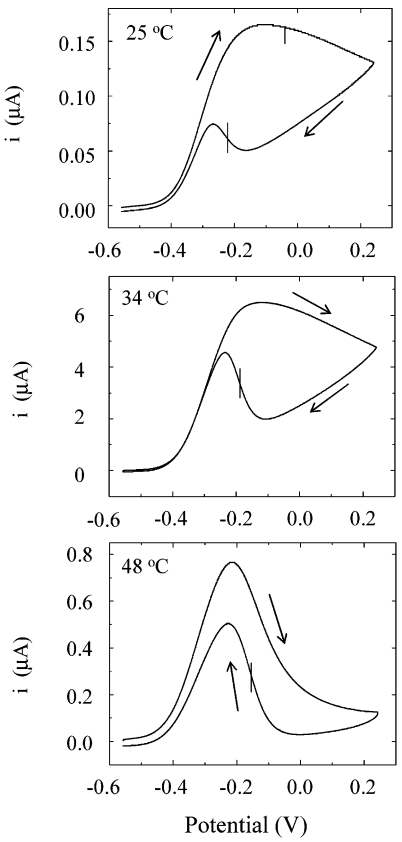

Figure 4. Cyclic voltammograms for a film of *Av*H_2ase measured at different temperatures as indicated. Other conditions: 1 bar H_2, scan rate 0.3 mV s^{-1}, rotation rate 2500 rpm, pH 8.8. The vertical bar on the curves indicates the position of E_{switch}. Arrows indicate the direction of the potential cycle.

to the presence of enzyme molecules that are adsorbed on the electrode.

The shape of the voltammetry changes dramatically as the scan rate is lowered, and Figure 2B shows that a peak-like response is obtained at 0.3 mV s^{-1}. This arises because the potential is scanned sufficiently slowly that there is now time for the enzyme to switch between active and inactive states (Scheme 1). As the potential is raised above the formal $2H^+/H_2$ value (ca. −0.52 V at pH 8.8), the H_2 oxidation current commences, as expected; but as the potential is increased further, the current drops. This inactivation is reversed (i.e., reactivation occurs) on the subsequent sweep back to a more negative potential. It is worth emphasizing again that the catalytic current relates *directly* to turnover rate, while changes in current translate as *changes* in turnover rate. The conditions used in this particular experiment, i.e., high pH and high temperature, accentuate this observation by optimizing the rates of transformations between states, while, as discussed below, other conditions produce considerable hysteresis in the cyclic voltammograms. The enzyme film is less stable than observed at lower temperature and pH, and typically about 30% is lost during the cycle (ca. 90 min). Figure 2C shows the derivative (d*i*/d*E*) of the reductive sweep of Figure 2B and depicts the parameter E_{switch} that we will adopt to define the characteristic potential for anaerobic interconversion between inactive and active states.

Influences of pH, Temperature, and H_2 Partial Pressure. Figure 3 shows how the shapes of slow cyclic voltammograms vary with pH. These were each measured under an atmosphere of 1 bar H_2 at 48 °C. As the pH is lowered, less inactivation is observed during the sweep to positive potential. By contrast, in every case, the sweep to negative potential produces a sharp rise in current and a well-defined peak, as enzyme molecules that have been switched off *reactivate*, with kinetics that are fast with respect to the scan rate. Oxidative inactivation is thus slow compared to reductive activation, and this irreversibility is much more marked at low pH.

Figure 4 shows the effect of temperature on the catalytic waveforms measured at pH 8.8. At the lower temperatures, the persistence of the H_2 oxidation current at high potential shows that the inactivation is much slower, and similar observations were made in experiments carried out at other pH values. As the temperature is raised, there is a significant positive shift in the potential of the peak observed during the scan in the negative direction, accompanied by a shift in E_{switch}. The voltammogram measured at 48 °C is for a film of lower coverage, hence, the smaller current; but the trend in peak position and E_{switch} (quantified later) was not dependent on enzyme coverage.

The cyclic voltammograms displayed in Figure 5 reveal how activation and inactivation vary with H_2 partial pressure at two different temperatures. Both sets of experiments were carried out at pH 8.8, cycling the potential under 0.01 bar H_2, then re-equilibrating the atmosphere at 1 bar H_2 and recording a second cyclic voltammogram without disturbing the enzyme film on the electrode. The smaller current observed in the experiment carried out at 45 °C arises because the coverage is lower than that at 25 °C. In either case, the experiments with 0.01 bar H_2 reveal only a small negative shift in the reactivation peak

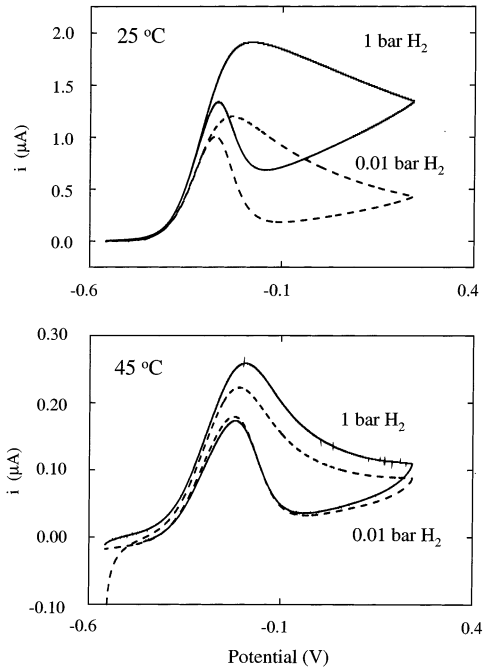

Figure 5. Effect of H_2 partial pressure on the appearance of cyclic voltammograms recorded at 0.3 mV s^{-1}, pH 8.8, at two different temperatures. (Upper panel) 25 °C: broken line, 0.01 bar H_2 (rotation rate 2500 rpm); black line, 1 bar H_2 (rotation rate 1500 rpm). (Lower panel) 45 °C: broken line, 0.01 bar H_2 (rotation rate 2500 rpm); black line, 1 bar H_2 (rotation rate 2500 rpm). All voltammograms were initiated from a potential of −570 mV.

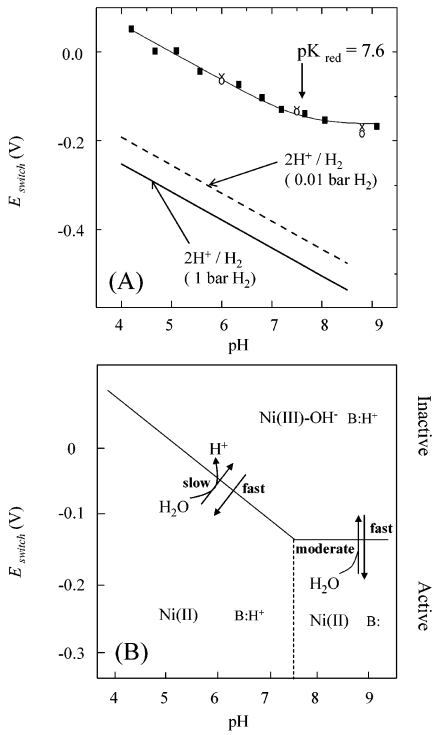

Figure 6. (A) Graph of the pH dependence of E_{switch} as obtained by taking the derivative of the reductive scans of cyclic voltammograms recorded for films of *Av*H_2ase at a slow scan rate (0.3 mV s^{-1}) and electrode rotation rate 2500 rpm. Squares depict values from experiments carried out at 45 °C under 1 bar H_2. Crosses and open circles represent experiments carried out at 48 °C under 1 bar H_2 or 0.01 bar, respectively. The modeled line for E_{switch}, using the 1 bar H_2 data, and the pH dependence of the $2H^+/H_2$ couple at 1 and 0.01 bar H_2 are also shown. The fit to eq 1 gives pK_{red} = 7.6 and E_{switch}^{alk} = −162 mV. (B) The resulting Pourbaix diagram showing the species and reactions implicated in these studies.

potential (and E_{switch}) compared to those carried out at 1 bar H_2. The higher H_2 partial pressure appears to retard inactivation, and this was confirmed using chronoamperometry, as described later. Before the onset of inactivation, that is, in the region between −500 and −250 mV, the catalytic current observed under 0.01 bar H_2 is only slightly lower than that for 1 bar H_2; this is as expected, since the K_M for H_2 is estimated to be in the micromolar range[9] (0.01 and 1 bar H_2 give solution concentrations below 8 μM and 800 μM, respectively).

Figure 6A shows how E_{switch} depends on pH, for experiments carried out at 45 °C, under 1 bar H_2. There was no significant variation in E_{switch} among different film preparations; nor was there any dependence on the oxidative potential limit of cyclic voltammograms or any effect of a 10-min pause holding the potential at the oxidative limit (242 mV, data not shown). The plot includes data obtained under 0.01 bar H_2 (measured at 48 °C; corresponding data for 1 bar H_2 at 48 °C also given). Shown also are the theoretical lines for the dependence of the formal $2H^+/H_2$ potential at 0.01 and 1 bar H_2. The data for E_{switch} were fitted to eq 1, in which R is the gas constant, T is the absolute temperature, F is the faraday constant, a_{H^+} is the proton activity obtained directly from the pH, K_{red} is the proton dissociation constant for the reduced form, n is the number of electrons transferred, and E_{switch}^{alk} is the limiting value of E_{switch} at pH values higher than pK_{red}.

$$E_{switch} = E_{switch}^{alk} + \frac{2.3RT}{nF}\log(1 + a_{H^+}/K_{red}) \qquad (1)$$

Equation 1 applies to a proton-coupled redox reaction for which the proton/electron stoichiometry is 1.0 under acid conditions ($\ll$pK_{red}) and 0 under basic conditions ($\gg$pK_{red}). We used n = 1 (see later discussion), and a good fit was obtained using E_{switch}^{alk} = −162 mV and pK_{red} = 7.6.

Rates of Activation and Inactivation. A potential-step technique, chronoamperometry, was used to study the time courses of activation and inactivation.[46] This method overcomes the convolution of potential and time variables that are a shortcoming of cyclic voltammetry. A typical potential step (or "pulse") sequence used to study inactivation is shown in Figure 7A. After forming a film of enzyme, then incubating under 1 bar H_2 for 1 h while holding the electrode potential at −558 mV, the potential is stepped to a more positive value and held there for 600 s, during which time the decrease in current (i) is recorded. After a constant current is reached, the potential is then stepped back to −558 mV for 60 s to reactivate the enzyme and then stepped up to a new value, and the current decay is again recorded. This is repeated several times, in each case increasing the potential used to drive inactivation. The resulting current−time profiles for experiments carried out at pH 8.8 are shown in Figure 7B, from which it is clear that there is little difference in the rate of current decrease as the potential is varied over the range −1 to 142 mV. This is reinforced in plots of log(current change) against time: these are shown in Figure 7C, which includes also the result of an experiment conducted with a much smaller driving force (potential −158 mV, close to E_{switch}). Apart from differences in the extent of inactivation (the trace at −158 mV obviously has a much smaller amplitude), the time courses for different potentials are almost identical and reproducible between films: notably, all

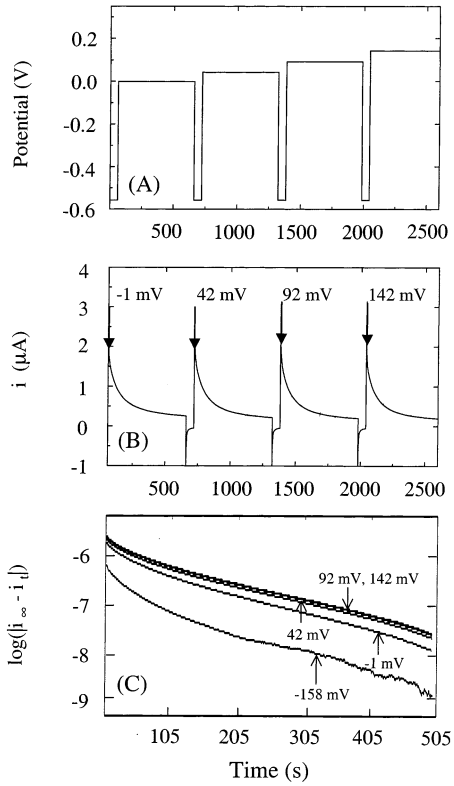

Figure 7. (A) Potential-step sequence used for chronoamperometric experiments to measure rates and potential dependence of inactivation of *Av*H_2ase. The film was first exposed to a reducing potential to activate the enzyme and then subjected to a series of oxidizing and reducing potentials to inactivate and reactivate the enzyme, respectively. (B) The current−time traces from a series of chronoamperometric experiments were carried out using the potential-step sequence shown in the top panel. Experimental conditions were pH 8.8, temperature 45 °C, electrode rotation rate 2500 rpm, and 1 bar H_2. (C) Overlay of semilog plots (log($|i_\infty - i_t|$) vs time, where i_∞ is the current measured when the reaction appears complete and i_t is the current at a particular time) for the inactivation traces at different potentials shown in the middle panel, showing how the rate is independent of potential. The trace for another experiment, conducted with a smaller driving force (−158 mV), is also included.

traces display some deviation from first-order behavior, with curvature (a higher rate constant for inactivation) observable even after the first 10 sec (the period of nominal "deadtime" where slow electrode charging contributes; see Materials and Methods).

The same kind of experiment was used to measure how the rate of inactivation depends on pH and H_2 partial pressure. Figure 8 shows the results obtained for experiments carried out at pH 7.0 and pH 8.8 (45 °C) where in either case the H_2 partial pressure was switched between 0.01 and 1 bar in consecutive runs on the same film of enzyme. The results are plotted as log(current change) against time (where the slope gives the rate constant) to extract the kinetics and detect small changes in rate. For pH 7.0, the experiments were performed in the order (1) 0.01 bar, (2) 1 bar, and (3) 0.01 bar, while, for pH 8.8, they were performed in the order (1) 0.01 bar, (2) 0.01 bar, (3) 1 bar, and (4) 1 bar. The results confirm that inactivation is slower at lower pH and slightly slower under 1 bar H_2. Again, deviations from first-order behavior are observed during the first minute of reaction.

Figure 9 shows the results of chronoamperometric experiments to observe the potential dependence of reductive activation. In each case, the enzyme was first inactivated by stepping

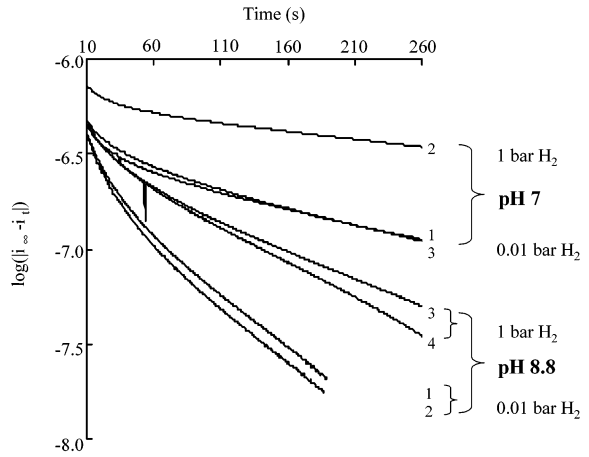

Figure 8. Semilog plots (log($|i_\infty - i_t|$) vs time) derived from chronoamperometric experiments performed to compare the rates of inactivation under 1 and 0.01 bar H_2 at two different pH values (7.0 and 8.8). In each case, the potential was stepped from −570 mV to +242 mV vs SHE to observe inactivation. The data at each pH were collected in consecutive experiments on the same enzyme film (one film was used to collect the pH 7.0 data, and another film was used to collect the pH 8.8 data). See text for details. Other experimental conditions were temperature 45 °C and electrode rotation rate 2500 rpm.

the potential to a positive value (100 mV higher than E_{switch}) for 10 min; then the potential was stepped back to a more negative value to induce activation, which was monitored (Figure 9A). This was repeated several times on the same film to study a range of driving forces. Reductive activation at pH 8.8, 45 °C, was studied over the potential range −148 to −288 mV, corresponding to values both above and below E_{switch}. To facilitate comparisons for each potential value, the amplitudes have been normalized with respect to the currents measured at the beginning of the 10-min inactivation step, to compensate for film loss. By contrast with oxidative inactivation, reductive activation shows a strong dependence on driving force; thus as the potential is lowered (raising the driving force for activation), the activation rate increases. The different amplitudes for each run are in accordance with respective catalytic currents expected from inspection of the voltammetric peak (see inset). Figure 9B shows the corresponding semilog plots. Neglecting the first 10 sec after the potential step, we found the traces to show fairly good linearity for several half-lives, consistent with a single-exponential process. While the reaction at lowest driving force shows the greatest curvature, that carried out at −288 mV is clearly complete within the 10-sec nominal deadtime, so that only a lower limit could be obtained for the rate constant. Similar experiments were carried out at pH 6.0: under these conditions, the rates were comparable to those observed at pH 8.8, and, again, generally first-order kinetics were observed, with the rate constant increasing with driving force. These data are not considered further in this paper, as more detailed investigations are currently underway to establish the exact form of the driving force dependence at different pH values.

Values of the entropy (ΔS) and enthalpy (ΔH) changes for the activation reaction were obtained by measuring the temperature dependence of E_{switch}.[49] Equation 2 is derived easily from the standard thermodynamic relationships between ΔH, ΔS, free energy ΔG, and reduction potential; therefore ΔS is

(49) Compton, R. G.; Sanders, G. H. W. *Electrode Potentials;* Oxford Science Publications Bath Press: Avon, UK, 1998.

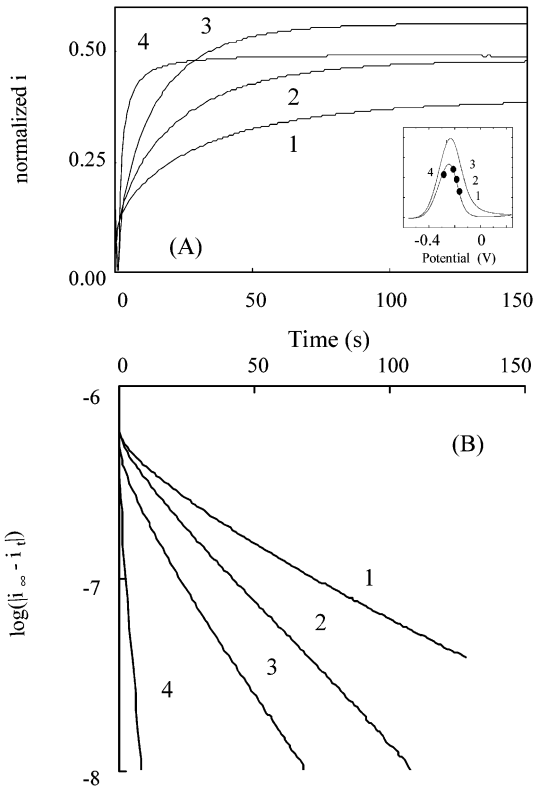

Figure 9. Chronoamperometric experiments to measure the time course of reductive reactivation as a function of potential. The enzyme was first inactivated at −68 mV for 600 s, and then the potential was stepped to different values to initiate reactivation. Experimental conditions were pH 8.8, temperature 45 °C, electrode rotation rate 2500 rpm, and 1 bar H_2. (A) Actual data obtained for four different potential steps: 1, −168 mV; 2, −188 mV; 3, −208 mV; 4, −288 mV. To compare traces for each potential value, we normalized the amplitudes with respect to the currents measured at the beginning of the inactivation step, to compensate for film loss. Inset shows a voltammogram measured under similar conditions indicating (●) final values of the potential steps made starting from −68 mV and the current amplitude expected in each case. (B) The corresponding semilog plots ($(\log(i_\infty - i_t)$ vs time). Reaction 4, induced with the highest driving force, is complete within 10 seconds, i.e., within the nominal "dead time". Rate constant estimates based on gradients are 1, 0.021 s^{-1} (only a guide since the line is curved); 2, 0.035 s^{-1}; 3, 0.052 s^{-1}; 4, >0.55 s^{-1}.

determined directly from the slope of a plot of E_{switch} against temperature.

$$E_{switch} = \frac{T\Delta S}{nF} - \frac{\Delta H}{nF} \qquad (2)$$

Figure 10A shows plots of E_{switch} against temperature, using data measured at pH values above and below the pK determined from Figure 6. A value of $n = 1$ was used, based upon considerations discussed below.

In all cases, data obtained between 25 °C and 48 °C conformed well to the expected linear relationship (although experiments carried out at 10 °C gave data points lying above the corresponding lines, suggesting that a different reaction is contributing at low temperature). Since slow kinetics and poor equilibration were likely to present problems at low temperatures, this observation was not investigated further in this study. Values of ΔH were determined from the slope of a plot of E_{switch}/T against $1/T$, which is shown in Figure 10B. Values of ΔS and ΔH, respectively, are as follows: (pH 8.8) 193 ± 39 J K^{-1} mol^{-1}, 78 ± 11 kJ mol^{-1}; (pH 7.5) 261 ± 53 J K^{-1} mol^{-1}, 95 ± 15 kJ mol^{-1}; (pH 6.0) 290 ± 48 J K^{-1} mol^{-1}, 96 ± 15 kJ mol^{-1}.

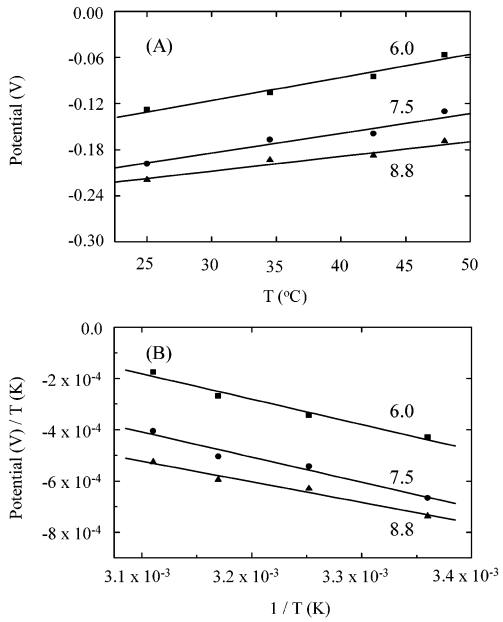

Figure 10. Plots showing the temperature dependence of E_{switch} values. Plot A is used to determine ΔS, and plot B is used to determine ΔH. All data were obtained under conditions of 1 bar H_2 and electrode rotation rate 2500 rpm. The pH values for each data set are indicated.

Discussion

These studies yield thermodynamic and kinetic data on transformations between active and inactive forms of a [NiFe]-hydrogenase that are difficult to obtain by conventional methods yet essential for a satisfactory understanding of the underlying chemistry. In terms of the effect it has on the catalytic *current*, the interconversion represents a *switch* that can be turned "on" or "off". It is important to consider the implications of these voltammetric experiments in light of what is already known of the properties of standard [NiFe]-hydrogenases obtained with other techniques; spectroscopy, redox titrations, activity measurements, and X-ray diffraction.

Evidence That the Interconversion Involves Ni_r* Rather Than Ni_u*. Spectroscopic methods have identified two most-oxidized, inactive states of the enzyme, that is, the Ni_u* and the Ni_r* states (see Scheme 1 for a summary of the known redox states of *Av*H_2ase).[8,23,25,33] In studies of the enzyme in solution, activation of the Ni_u* state by H_2 is known to require reduction for more than 30 min at 50 °C (although higher rates are reported with reduced methyl viologen), whereas activation of Ni_r* is a much faster process.[9] Therefore, the observation that inactive enzyme on the electrode can be almost completely reactivated within a few seconds (Figure 9) suggests strongly that oxidative inactivation of *Av*H_2ase on the electrode surface results in formation of Ni_r* rather than Ni_u*. This is consistent with the observation that only Ni_r* is formed by oxidation of the *A. vinosum* enzyme at high pH values.[24] The fact also that the enzyme has been preactivated under H_2 leads us to conclude that Ni_u* is not being addressed to any significant extent in these studies. Despite the absence of spectroscopic evidence (the quantity of enzyme being addressed is $\ll 10^{-12}$ mole), the only reasonable inference is that the major product of anaerobic

inactivation on the electrode is Ni_r*. Referring to Scheme 1, the product of activation is necessarily a participant of the very rapid catalytic cycle, and since the actual process of activation is relatively slow, it follows that its "end-product" cannot be defined further. We propose therefore that the electrochemical experiments are addressing the interconversion between a fully active state (Ni_a) and the oxidized inactive "ready" state Ni_r*. Below, we discuss the likelihood that the Ni_a "end-product" species is Ni_a-S.

Voltammetry of *Av*H_2ase at low scan rates reveals a marked hysteresis between the oxidative and reductive scans. While it has been noted previously from solution studies that oxidative inactivation is much slower than reductive activation,[8] our electrochemical experiments provide a more precise assessment since they allow the interconversions to be controlled directly and linked to the electrode potential. Oxidative inactivation is faster at high pH (see Figures 3 and 8), and in this case it is clearly observed at a potential that is close to that observed for reductive activation. We therefore conclude that E_{switch} is a robust parameter, for which we may attach thermodynamic significance at high pH and be confident that it has, at least, an empirical significance at lower values. While others have reported that [NiFe]-hydrogenase (from *D. gigas*) is not inactivated in the presence of H_2,[10] our results provide a more critical and quantitative assessment of this protection effect. Not only is there no doubt that the enzyme can be inactivated in the presence of H_2, but it is clear from Figures 5 and 8 that increasing the H_2 pressure from 0.01 to 1 bar causes only a small retardation of rate and hardly alters E_{switch}.

pH Dependence and Assignment of Species Involved. The pH dependence of the data shown in Figure 6A is also represented in Figure 6B in the form of a Pourbaix diagram, which indicates the species taking part. As discussed later, Figure 6B also includes an internal base 'B' that is implicated in the transformations. Below pK_{red} the slope shows that H^+ and e^- are transferred in a 1:1 ratio. Since we were unable to determine the absolute number of electrons in the (in)activation process by analysis of the voltammetric waveshapes (there are too many variables), there remains the possibility that a second electron is always required, most obviously to reduce the medial [3Fe−4S] cluster. However, this center has a much higher reduction potential (−30 mV at pH 7.0), while the two [4Fe−4S] clusters are more reducing (ca. −300 mV).[41] From the results, there is good reason to propose that the transformation involves only one electron, since if there were cooperative uptakes of two (or even more) electrons accompanied by the same number of protons (thus retaining the 1:1 ratio at pH < p*K*), it would be necessary to invoke a situation at high pH (pH > pK_{red}) in which these electrons are transferred to the active site without any compensation from proton transfer (since the gradient is zero in this region). On electrostatic grounds, this is very unlikely and we propose instead that the transformation at low pH involves one electron and one proton. This is as reported by Mege and Bourdillon[10] who titrated the activity of *D. gigas* hydrogenase using methyl viologen; although an acid−base transition (pK_{red}) was not observed in that study.

The most persuasive assignment for the reduced states in our experiments is that they are pH-interconvertible forms of Ni_a-S. First, the results are consistent with recent studies[44] of the catalytic electrochemistry of the *A. vinosum* enzyme, in which an acid−base transition p*K* 7.4 is associated with the active enzyme in its most oxidized state. Second, FTIR-spectroelectrochemical measurements on *D. gigas* hydrogenase[18] have suggested that Ni_a-S exists in two forms, Ni_a-S_{1914} and Ni_a-S_{1934} (our terminology), depending on pH, with a p*K* of around 8.2. In that investigation, Fernandez and co-workers obtained a value of −150 mV at pH 8.0 for the midpoint potential of the couple Ni_r*/Ni_a-S, while Roberts and Lindahl determined a value of −140 mV (pH 8.0) using EPR.[12] There are variations among different measurements: methyl viologen titrations of *D. gigas* hydrogenase yielded a value of −210 mV for the transition potential at 25 °C, pH 8.3,[10] while an earlier EPR titration of the Ni_r* state in the *A. vinosum* enzyme produced a value of −115 mV for a one-electron reaction at pH 8.0, 30 °C.[8] But in general, there are broad correlations between our voltammetric activity data ($E_{switch}^{alk} = -162$ mV, p$K_{red} = 7.6$) and titrations that focus spectroscopically on Ni_r* and Ni_a-S.

Correlations with Structurally Defined States. The pH dependence of reduction potentials can be correlated with previous X-ray structural and spectroscopic studies. The crystal structure determined for an oxidized form of [NiFe]-hydrogenase from *D. gigas* revealed the presence of a bridging ligand between the Ni and Fe atoms.[16,18,20] The earlier-mentioned EPR and ENDOR spectroscopic studies with ^{17}O demonstrate that an O atom, derived either from $^{17}O_2$ or from $H_2{}^{17}O$, is bound to Ni(III).[13,14] It has been proposed further, on the basis of proton hyperfine coupling results, that Ni_r* might contain a *terminal hydroxo* ligand, while Ni_u* has a *bridging oxo* ligand (Figure 1).[24] This would explain why activation of Ni_u* is so slow. However, recent X-ray structural studies[50] and density functional calculations[34] indicate that both Ni_u* and Ni_r* contain a bridging O species, so the situation remains unclear. The dependence of E_{switch} on pH shows that oxidation of active Ni_a-S to inactive Ni_r* involves uptake of a hydroxo ligand (or equivalently the removal of a proton from a nearby base in the active site) and that, at high pH, activation occurs *without* a simultaneous proton transfer from the solvent. The simplest interpretation is that Ni(III) is present as an OH^- species throughout the entire pH range: reduction at pH < pK_{red} results in an Ni(II) species that no longer contains the OH^-, whereas, at pH > pK_{red}, the lack of a proton exchange during electron transfer suggests that the OH^- ligand either is retained in the Ni coordination sphere or is released after combining with a nearby proton. It is important to note that the inherent activity for H_2 oxidation remains high at pH > pK_{red}.[44]

The large positive ΔS and ΔH values are indeed consistent with Ni_r* containing a tightly bound bridging group that is released to solvent during activation. (Alternatively, there may be some partial unfolding or relaxation of the structure around the active site, but release of a bridging group is certainly inferred from the spectroscopic and structural studies.[15−22,51]) This is particularly the case at lower pH values, for which ΔS and ΔH are somewhat higher than those at pH 8.8 (although the differences lie only just outside the error margins). In absolute terms, the activation process at higher pH is still associated with a large positive ΔS: this suggests that above

(50) Volbeda, A.; Matho, M.; Martin, L.; Cavazza, C.; Faber, B.; Albracht, S. P. J.; Fontecilla-Camps, J. C. Manuscript in preparation.
(51) Davidson, G.; Choudbury, S. B.; Gu, Z.; Bose, K.; Roseboom, W.; Albracht, S. P. J.; Maroney, M. J. *Biochemistry* **2000**, *39*, 7468−7479.

pK_{red} the coordinated OH^- is still released but is ejected instead as a water molecule after extraction of a proton from a nearby internal donor. In Figure 6B, the internal base or proton donor (yet to be identified) is represented as B: or $B:H^+$ respectively.

Two-Stage Mechanism and Intermediate State. The kinetic studies provide the following facts. First, reductive activation is a first-order process for which the rate constant increases with the electrochemical driving force: this is consistent with a reaction that is driven directly by an electron transfer. Second, the rate of the reverse reaction, oxidative inactivation, is potential-*independent* over a range of 300 mV (Figure 7C), and therefore consistent with a controlling *chemical* event: the reaction is also slower at low pH. We note further that the inactivation kinetics deviate from first-order behavior (in contrast to activation) and this suggests the possibility that active enzyme displays heterogeneity with regard to the ease of undergoing inactivation. This is currently under further investigation. As now discussed, the general pattern of electrochemical asymmetry arises from participation of a reduced intermediate state. Formally, the results are explained by the following sequence of events, given by eqs 3 and 4A, involving electrochemical (E) and chemical (C) steps.[46]

$$\underset{\text{(inactive)}}{Ni^{III}-OH^-} + e^- \rightleftharpoons \underset{\text{(inactive)}}{Ni^{II}\sim OH^-} \quad = E \tag{3}$$

$$\underset{\text{(inactive)}}{Ni^{II}\sim OH^-} \rightleftharpoons \underset{\text{(active)}}{Ni^{II} + OH^-_{out}} = C \tag{4A}$$

For activation, reduction of $Ni^{III}-OH$ (Ni_r*) is driven directly by the electrode potential (the rate increases as a more negative potential is applied) and followed by release of the OH^- ligand (in electrochemical terminology, this is called an "EC" reaction[46]) to yield Ni^{II} (Ni_a-S). By contrast, for inactivation, the rate-controlling process is the incorporation of OH^- into the active site, whereupon electron transfer follows rapidly to generate the product (this is a "CE" reaction). The inferred electrochemical intermediate $Ni^{II}\sim OH$ is likely to be Ni_r-S or a closely related species (see Scheme 1). There is evidence from X-ray spectroscopy[51] that Ni_r-S contains four-coordinate Ni and that the bridging O-donor ligand is no longer coordinated: therefore, the possibility that a noncoordinating OH^- is still retained in the active site in this intermediate state is represented by the symbol $\sim$. The likelihood that the protein facilitates transfer of H^+ (one of the substrates) and H_2O (neutral) more than the anion OH^- suggests further that eq 4A can be replaced by 4B, in which the quantity of $Ni^{II}-OH$ is inversely related to the H^+ concentration in solution.

$$\underset{\text{(inactive)}}{Ni^{II}\sim OH^-} + H^+ \rightleftharpoons \underset{\text{(active)}}{Ni^{II} + H_2O_{out}} = C \tag{4B}$$

The activation−inactivation cycle, starting from inactive enzyme, is therefore of the "EC/CE" type, so that the return cycle (inactivation) is slow except at high pH, thus accounting for the hysteresis that is observed.

A summary of the interconversions that we can infer from these studies is included in Figure 6B, and the electrochemical relationship between Ni_r* and the catalytic cycle is depicted in

Scheme 2. Scheme Depicting the Electrochemical Reaction Sequence Addressed in This Study

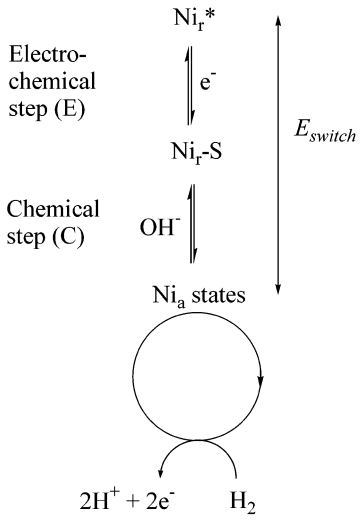

Scheme 2. The observation that neither E_{switch} nor the rate of inactivation is much affected by the partial pressure of H_2, at least over the 100-fold range 0.01−1 bar, is unambiguous, yet perhaps surprising since H_2 (as both a good reductant and substrate) should favor the generation and retention of active enzyme, at least on thermodynamic grounds. There is indeed a window of approximately 200 mV within which the enzyme can catalyze H_2 oxidation *without* undergoing oxidative inactivation. Clearly, many finer details remain to be addressed. We have assumed that E_{switch} is a good thermodynamic approximation for all our studies. We have not yet carried out experiments at much lower H_2 partial pressures to measure under conditions where the system is far from being saturated with substrate and might "escape" more easily from the catalytic cycle; we have not addressed the roles of the Fe−S centers that must relay the electron to activate the Ni site, insights into which may be afforded by detailed studies of the electrochemical driving force (free energy) dependence under different conditions.

In conclusion, the experiments we have described, which exploit the remarkable electrocatalytic activity of *Av*H$_2$ase and the control over the potential dimension that is acquired with protein film voltammetry, are able to resolve the entangled thermodynamics and kinetics of interconversion between active and inactive states of a [NiFe]-hydrogenase. More detailed studies are in progress, to follow up the questions raised above. Our lines of investigation complement the extensive spectroscopic and structural studies that have been underway for some time and should help to establish an improved framework for understanding and exploiting this class of enzymes.

Acknowledgment. We thank the UK EPSRC, BBSRC (43/E16711), and The Netherlands Organization for Scientific Research (NWO) division for Chemical Science for funding. A.K.J. thanks the Rhodes Trust and the National Science Foundation for scholarships. Mr. Winfried Roseboom is acknowledged for his help with enzyme preparation. We are grateful to Drs. Christophe Léger, Lars Jeuken, Hendrik A. Heering, Boris Bleijlevens, and Bart Faber for helpful discussions.

JA035296Y